Inorganic Chemistry

Article

pubs.acs.org/IC

Effect of Deuteration on the Thermodynamic Properties of Dioxotetrafluoromolybdate(VI), $(NH_4)_2MoO_2F_4$

Evgeniy V. Bogdanov,[†,‡] Evgeniy I. Pogoreltsev,*[,†,§] Mikhail V. Gorev,[†,§] and Igor N. Flerov[†,§]

[†]Kirensky Institute of Physics, Federal Research Center KSC SB RAS, 660036 Krasnoyarsk, Russia

[‡]Institute of Engineering Systems and Energy, Krasnoyarsk State Agrarian University, 660049 Krasnoyarsk, Russia

[§]Institute of Engineering Physics and Radioelectronics, Siberian State University, 660074 Krasnoyarsk, Russia

ABSTRACT: Thermal and dielectric studies of $(ND_4)_2MoO_2F_4$ crystals undergoing successive phase transitions at T_1 = 272 K and T_2 = 181 K showed that deuteration is accompanied by an increase in the chemical pressure in the crystal lattice ($\Delta p \approx 0.02$ GPa), which shifts the *Cmcm* ↔ *Pnma* transformation for the first order to the tricritical point. The direct participation of ammonium groups in the mechanism of structural distortions is demonstrated by a decrease in the entropy of the high-temperature phase transition ($\Delta S_1 = R \ln 6.0$). An external hydrostatic pressure leads to an expansion of the temperature interval of the intermediate antiferroelectric *Pnma* phase. The triple point on the $T-p$ phase diagram, where the *Cmcm*, *Pnma*, amd *Pnma** phases coexist, can be realized at a negative pressure of $p_{trp} \approx -0.8$ GPa.

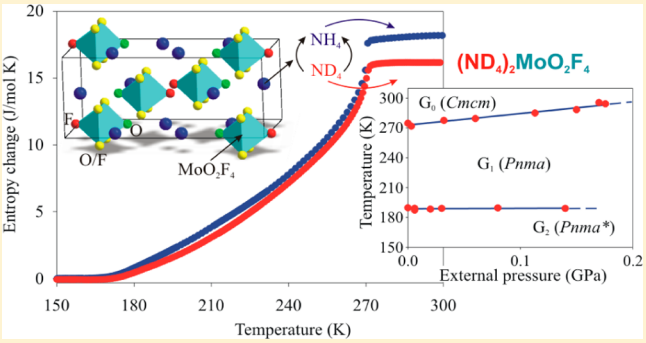

1. INTRODUCTION

The study of oxyfluoride compounds with octahedral anionic structural elements, in which a central atom is displaced toward oxygen ligands, is important in the search for polarization in the initial crystal phase and its appearance due to a change in the internal (chemical pressure) and/or external (temperature, external pressure, etc.) parameters.[1−3]

The recently studied crystals $AA'MeO_2F_4$ (A, A′ = NH_4, ND_4, K, Cs, Rb; Me = W, Mo) have an initial orthorhombic structure (space group *Cmcm*, Z = 4) consisting of isolated octahedra $[MeO_2F_4]^{2-}$ and two crystallographically nonequivalent A and/or A′ cations; these undergo successive phase transitions upon cooling: $G_0(T_1) \leftrightarrow G_1(T_2) \leftrightarrow G_2$.[4−6]

Substitution of the central atom Mo → W in ammonium compounds leads to a strong increase in the temperature of the $G_0 \leftrightarrow G_1$ transformation (T_1 = 200 K → 270 K), which is also accompanied by a change in both the symmetry ($P\bar{1}$ → *Pnma*, Z = 4) and the origin (ferroelastic → antiferroelectric) of the G_1 phase.[7] Structural distortions at the $G_1 \leftrightarrow G_2$ phase transition are apparently so small that X-ray diffraction does not allow the change in symmetry of $(NH_4)_2WO_2F_4$, $(ND_4)_2WO_2F_4$, and $(NH_4)_2MoO_2F_4$ to be determined.[4,7,8] Recent X-ray studies of $(ND_4)_2MoO_2F_4$ have assumed the existence of four possible variants of the symmetry of the G_2 phase: *Pnma*, $P2_12_12_1$, $Pmc2_1$, and $Pna2_1$;[9] in their deuterated analogues, these can be presented as G_0 (space group *Cmcm*) ↔ G_1 (space group $P\bar{1}$) ↔ G_2 (space group $P\bar{1}$*) and G_0 (space group *Cmcm*) ↔ G_1 (space group *Pnma*) ↔ G_2 (space group *Pnma**).

A study of the influence of the external hydrostatic pressure on the stability of the crystal phases in $(NH_4)_2MoO_2F_4$ showed, on the one hand, an almost 7-fold increase in the baric coefficient dT_1/dp = 92.7 K/GPa compared to $(NH_4)_2WO_2F_4$ and, on the other hand, a decrease in the value of dT_2/dp = 17 K/GPa of about 2.5 times. Thus, $(NH_4)_2MoO_2F_4$ is characterized by a strong expansion of the intermediate antiferroelectric phase (space group *Pnma*) with the pressure increase. Substitution of a central atom has shown that the *Pnma* phase is energetically more favorable in $(NH_4)_2W_{1-x}Mo_xO_2F_4$ solid solutions because this was realized in compounds with a wide range of molybdenum concentrations ($0.3 \le x \le 1.0$).[10]

This marked difference between the symmetry and properties of the G_1 phase of the related $(NH_4)_2WO_2F_4$ and $(NH_4)_2MoO_2F_4$ compounds is due to the different mechanisms of the structural distortions. A complete ordering of ligands and a partial ordering of ammonium groups was found in $(NH_4)_2WO_2F_4$, whereas in $(NH_4)_2MoO_2F_4$, the complete ordering of NH_4 groups was accompanied by a partial ordering of ligands.[5,6]

The active role of the ammonium groups in the mechanism of structural changes in $(NH_4)_2WO_2F_4$ has been demonstrated by a study of the deuterated analogue $(ND_4)_2WO_2F_4$ undergoing the same sequence of structural changes G_0 (space group *Cmcm*) ↔ G_1 (space group $P\bar{1}$) ↔ G_2 (space group $P\bar{1}$*).[8] Deuteration changed the temperatures of both

Received: March 31, 2017
Published: May 11, 2017

DOI: 10.1021/acs.inorgchem.7b00811
Inorg. Chem. 2017, 56, 6706−6711

phase transitions only slightly and also caused a substantial decrease in the entropy of the $Cmcm \leftrightarrow P\bar{1}$ transition (ΔS_1 = 18.9 → 13.2 J/mol·K). An investigation of the effect of the external hydrostatic pressure on $(ND_4)_2WO_2F_4$ showed the value of the pressure coefficient $dT_1/dp \approx 13.3$ K/GPa to be almost unchanged, while a strong increase in the value of dT_2/dp = 41.7 → 112.3 K/GPa was observed. As a result, a triple point was found at $p \approx 0.18$ GPa, where the intermediate phase $P\bar{1}$ disappears.

In the present paper, we continue to explore the succession of phase transitions recently found in $(ND_4)_2MoO_2F_4$.[9] Complex studies of the heat capacity, entropy, thermal expansion, susceptibility to external pressure, and dielectric properties were performed in order to shed light on the role of ammonium groups in the mechanism and the nature of the phase transitions.

2. EXPERIMENTAL SECTION

2.1. Synthesis and Structure. In order to obtain the deuterated compound, the starting material of $(NH_4)_2MoO_2F_4$ was dissolved in heavy water (99.9% D). Then, the solution was placed in a desiccator with P_2O_5 until complete water absorption had taken place. The process of recrystallization in heavy water was repeated several times in order to obtain the maximum percentage of deuteration. The degree of deuteration, which was found to be 95%, was determined by comparing the integral NMR absorption of ^1H lines of the protonic and deuterated compounds.[9] X-ray diffraction (XRD) showed that the sample was a single phase and that deuteration did not change the original symmetry of the crystal at room temperature (space group *Cmcm*).

2.2. Specific Heat and Thermal Expansion. A precise determination of the temperature, excess heat capacity, and integral characteristics associated with phase transitions was carried out via measurements of the heat capacity of $(ND_4)_2MoO_2F_4$ using a homemade adiabatic calorimeter with two thermal shields.[11]

The sample, consisting of small single crystals with a total mass of 1.1 g, was hermetically packed in an indium capsule in an inert atmosphere of helium and placed in a heater. Calorimetric measurements were carried out using continuous ($dT/dt \approx 0.15$ K/min) and discrete ($\Delta T \approx 2.5$–3.0 K) modes of heating over a temperature range of 90–300 K. In the vicinity of the phase transition temperature, investigations were carried out using a method of quasi-static thermograms with an average heating of $dT/dt \approx 0.02$ K/min. The heat capacity of the equipment, consisting of the heater and indium capsules, was measured in a separate experiment.

On the basis of the temperature dependence of the molar isobaric heat capacity C_p of $(ND_4)_2MoO_2F_4$ (Figure 1a), more accurate phase transition temperatures were defined as follows: T_1 = 271.80 ± 0.05 K and T_2 = 181.3 ± 0.5 K. The temperature hysteresis δT_1 = 0.6 K of the G_1 (space group *Cmcm*) ↔ G_2 (space group *Pnma*) phase transition, determined using quasi-static thermograms (Figure 1b), was found to be equal to the value observed in the birefringence measurements.[9]

Separation of the total heat capacity C_p on a regular lattice C_L and anomalous ΔC_p contributions was carried out in order to determine the enthalpy and entropy of the phase transitions. For this purpose, the experimental data $C_p(T)$ taken far from the transition points (at T < 165 K and at T > 285 K) were fitted using a linear combination of Debye and Einstein terms; the equation $C_L = K_D C_D + K_E C_E$ models the temperature behavior of the excess heat capacity (Figure 2a). Integration of the $\Delta C_p(T)$ function over the entire range of existence of the excess heat capacity allowed the total change in the enthalpy associated with two phase transitions to be determined as $\sum \Delta H_i$ = 3900 ± 280 J/mol. The individual changes in the enthalpy ΔH_1 = 3650 ± 250 J/mol and ΔH_2 = 250 ± 50 J/mol were determined using the Landau thermodynamic theory (Figure 2b). The magnitudes of the entropy change $\Delta S_i = \int (\Delta C_p/T)\, dT$ associated with the transformations (*Cmcm* → *Pnma* and *Pnma* → *Pnma**) were determined as follows: ΔS_1 = 15 ± 1 J/mol·K and ΔS_2 = 1.2 ± 0.2 J/mol·K.

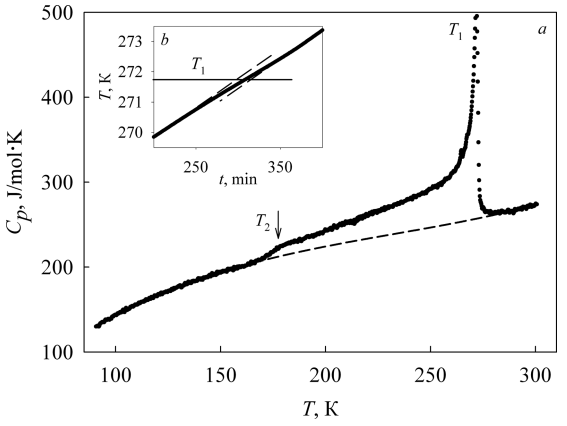

Figure 1. (a) Temperature dependence of the molar heat capacity of $(ND_4)_2MoO_2F_4$ in a wide temperature range. Dashed line: lattice specific heat. (b) Thermogram in the heating mode in the vicinity of T_1.

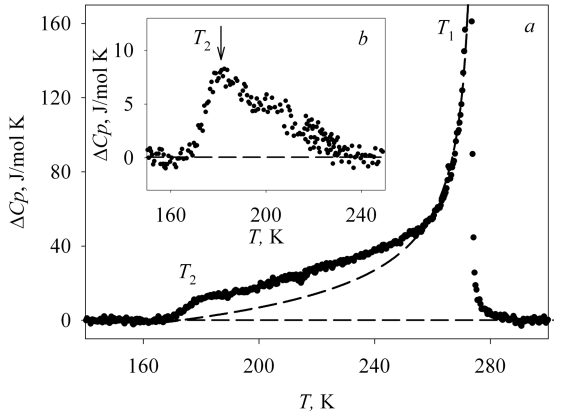

Figure 2. (a) Temperature dependence of the excess molar heat capacity of $(ND_4)_2MoO_2F_4$ associated with the phase transitions at T_1 and T_2. Dashed line: contributions separated into $\Delta C_p(T)$ values by using the Landau thermodynamic theory. (b) Temperature dependence of excess molar heat capacity at T_2.

The temperature evolution of the linear thermal expansion was recorded over a temperature range of 120–350 K using a Netzsch model DIL402C pushrod dilatometer in dynamic mode with a heating rate of 3 K/min. Investigations were carried out for a dry helium flux with a flow rate of ~50 mL/min. In order to take into account the thermal expansion of the system, calibration was carried out using quartz as the standard reference.

The samples of $(ND_4)_2MoO_2F_4$ for the dilatometric experiments were prepared as quasi-ceramic tablets with a diameter of 4 mm and a thickness of about 4–6 mm, by pressing at about ~2 GPa; heat treatment was not used because of the presence of ammonium ions. The temperature dependence of the volume deformation, $\Delta V/V_0 = 3(\Delta L/L_0)$, and the coefficient of the volumetric thermal expansion, $\beta = 3\alpha$, are shown in Figure 3a over a wide temperature range. $\Delta L/L_0$ is a linear deformation determined by direct dilatometric measurements, and $\alpha = \partial(\Delta L/L_0)/\partial T$ is the coefficient of linear thermal expansion.

The strain undergoes anomalous behavior in the region of both phase transitions: a poorly defined jump at T_1 and a kink at T_2 (Figure 3b). The temperatures of the maximum values of the expansion coefficient β, considered to be the phase transition temperatures T_1 = 274 ± 1 K and T_2 = 183 ± 2 K, are close to the temperatures defined by the calorimetric measurements.

2.3. Sensitivity to the Hydrostatic Pressure. The effect of the hydrostatic pressure on the phase transition temperatures in $(ND_4)_2MoO_2F_4$ was studied by differential thermal analysis (DTA).

DOI: 10.1021/acs.inorgchem.7b00811
Inorg. Chem. 2017, 56, 6706–6711

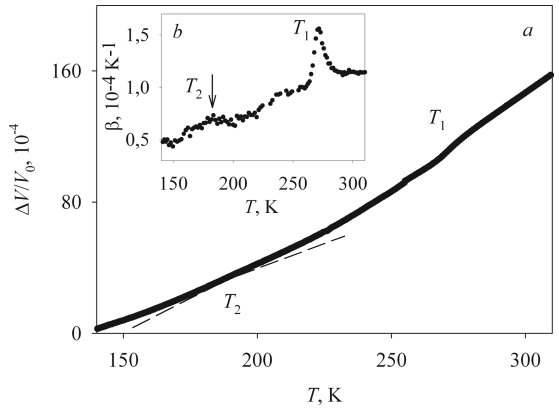

Figure 3. (a) Temperature dependence of the spontaneous deformation strain. (b) Temperature dependence of the coefficient of volume expansion.

A polycrystalline sample with a mass of ~0.025 g was placed in a copper container, which was glued onto one of two junctions of a germanium−copper thermocouple characterized by a high sensitivity to changes in temperature. A quartz sample cemented to the other junction was used as the reference substance. Experiments with the hydrostatic pressure were carried out using a piston−cylinder-type vessel associated with a pressure multiplier. Pressure was generated using silicone oil as the pressure-transmitting medium. The temperature and pressure were measured using a copper−constantan thermocouple and a manganin gauge, with accuracies of about ±0.3 K and $\pm 10^{-3}$ GPa, respectively.

The stability of the initial and distorted crystal phases in $(ND_4)_2MoO_2F_4$ changes under hydrostatic pressure, as can be seen in the T–p phase diagram (Figure 4). An increase in the pressure is

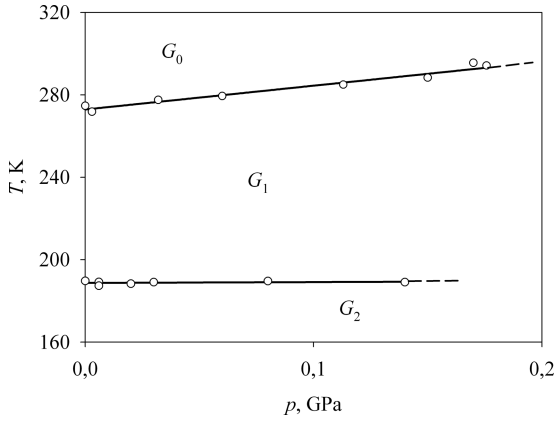

Figure 4. Temperature−pressure phase diagram of a crystal of $(ND_4)_2MoO_2F_4$.

accompanied by a decrease in the DTA anomalies, which become very blurred and undetectable at a pressure of $p \geq 0.2$ GPa. To ensure the reliability of the results, the measurements were performed under both increasing and decreasing pressures. The temperature range of the stability of the initial phase G_0 (space group *Cmcm*) narrows with an increase in the pressure (Figure 4), which is associated with the relatively high rate of rise in the T_1 temperature (dT_1/dp = 115 K/GPa). The susceptibility of T_2 (*Pnma* → *Pnma**) to a pressure increase is significantly lower (dT_2/dp = 4 K/GPa).

2.4. Dielectric Properties. A study of the dielectric properties was carried out using an E7-20 LCR meter at a frequency of 1 kHz, involving heating and cooling at a rate of about ~0.7 K/min in a temperature range of 100−320 K. Measurements were performed on the samples used previously in dilatometric experiments with gold electrodes deposited in a vacuum.

Figure 5a shows the temperature dependence of the dielectric constant (ε) and the tangent of the dielectric loss (tan δ) measured in

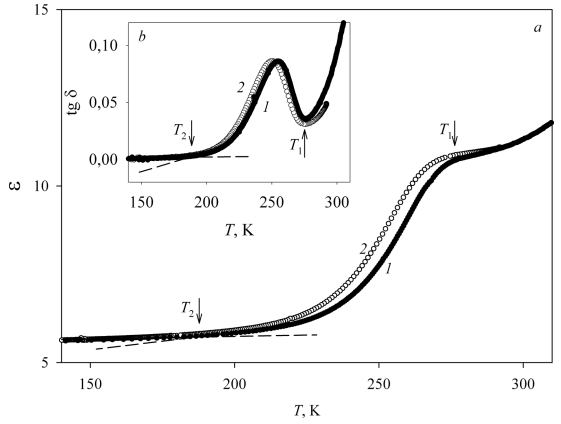

Figure 5. Temperature dependence of the (a) permittivity and (b) dielectric losses on the heating (1) and cooling (2) modes.

both heating and cooling modes. Upon heating, a detectable increase in the permittivity begins at about T_2 and reaches a plateau in the region of T_1. The temperature dependence of tan δ (Figure 5b) is also characterized by complicated anomalous behavior. Initially, the dielectric loss increases up to about 255 K; it then quickly decreases to T_1 = 273 K and finally increases again. Both the functions $\varepsilon(T)$ and tan $\delta(T)$ show hysteretic phenomena over a broad temperature range below T_1; this is primarily due to dynamic mode measurements.

3. ANALYSIS AND DISCUSSION

Recent X-ray and optical investigations[9] have shown that the succession of phase transitions in $(ND_4)_2MoO_2F_4$ is similar to that found earlier in $(NH_4)_2MoO_2F_4$.[7] Moreover, deuteration is accompanied by a rather small change in the temperature of the structural transformations. On the other hand, the decrease in hysteresis of the T_1 temperature δT_1 = 0.9 K (NH_4) → 0.6 K (ND_4) found from both optical experiments[9] and the calorimetric measurements in the present paper shows that the first-order phase transition *Cmcm* ↔ *Pnma* in $(ND_4)_2MoO_2F_4$ is closer to the tricritical point. This is also demonstrated by a decrease in the ratio between the jump and the complete change in the entropy ($\delta S_1/\Delta S_1$) at T_1 (Table 1).

Another parameter characterizing the proximity of the transformation to the tricritical point is the quantity N =

Table 1. Thermodynamic Parameters of the Phase Transitions in $(NH_4)_2MoO_2F_4$[7] and $(ND_4)_2MoO_2F_4$ Crystals (R is the Gas Constant)

parameter	$(NH_4)_2MoO_2F_4$	$(ND_4)_2MoO_2F_4$
T_1, K	270	272
$\Delta S_1/R$	ln 8.9	ln 6.0
$\delta S_1/\Delta S_1$	0.11	0.04
dT_1/dp, K/GPa	93	116
A_T^2/B, J/mol·K^2	− 0.7	− 1.7
A_T^3/C, J/mol·K^3	16.4	7.2
$T_1^* - T_1$, K	1.4	0.2
$T_1 - T_C$, K	4.2	0.6
N	−0.18	−0.05
T_2, K	180	181
$\Delta S_2/R$	ln 1.2	ln 1.2
dT_2/dp, K/GPa	17	4.0

DOI: 10.1021/acs.inorgchem.7b00811
Inorg. Chem. 2017, 56, 6706−6711

$\pm(B^2/3A_TCT_0)^{-0.5}$.[12] Here, T_0 is the temperature of the phase transition, and A_T, B, and C are the coefficients of the thermodynamic potential $\Delta\Phi(p,T,\eta) = [A_T(T_0 - T_C) + A_T(T - T_0)]\eta^2 + B\eta^4 + C\eta^6$, where η and $T_C = T_0 - B^2/4A_TC$ are an order parameter and the Curie temperature, respectively.

According to Landau thermodynamic theory, the value of $(\Delta C_p/T)^{-2}$ is a linear function of the temperature below the phase transition point:[12]

$$\left(\frac{\Delta C_p}{T}\right)^{-2} = \left(\frac{2\sqrt{B^2 + 3A'C}}{A_T{}^2}\right) + \frac{12C}{A_T{}^3}(T_0 - T)$$

As seen in Figure 6, the temperature behavior of the excess heat capacity of $(ND_4)_2MoO_2F_4$ follows a linear dependence

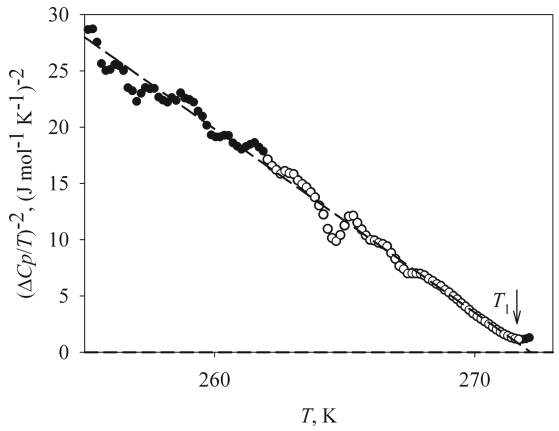

Figure 6. Temperature dependence of the square of the inverse excess heat capacity of $(ND_4)_2MoO_2F_4$.

over a fairly wide range of temperature, $T_1 - T \approx 15$ K; this allows us to define the relationship between the coefficients of the thermodynamic potential. Table 1 shows that D → H substitution leads to a significant change in the values of $A_T{}^2/B$, $A_T{}^3/C$, $T_1{}^* - T_1$, and $T_1 - T_C$. Here, $T_1{}^*$ is the temperature at which the value of $(\Delta C_p/T)^{-2}$ becomes zero because of the approach of the first-order phase transition *Cmcm* ↔ *Pnma* to the tricritical point. This point is most clearly demonstrated by a strong decrease in the modulus of the N value.

The entropy of the *Cmcm* ↔ *Pnma* phase transition in $(ND_4)_2MoO_2F_4$ remains characteristic of the order−disorder transformation (Table 1 and Figure 7) despite a decrease of about 20% compared to $(NH_4)_2MoO_2F_4$. Deuteration of the compounds $(NH_4)_2WO_2F_4$ was also accompanied by a decrease in the entropy of ∼30%.[8] It would be useful to compare these values of ΔS_1 with the entropy of transformation for a related compound with a monoatomic cation. Recent X-ray and calorimetric studies have shown that $Rb_2MoO_2F_4$ also undergoes this succession of two-phase transitions; however, the symmetry of the distorted phases is similar to those in $(NH_4)_2WO_2F_4$.[13] Nevertheless, it is interesting that the entropy change at the *Cmcm* ↔ $P\bar{1}$ phase transition in $Rb_2MoO_2F_4$ was found to be relatively large (ΔS_1 = 9.2 J/mol·K ≈ R ln 3). This value is close to R ln 3.3, which has been suggested as a contribution to ΔS_1 associated with the ordering of central atoms in $(NH_4)_2WO_2F_4$.[5] In accordance with a structural model, it was assumed that only 86% of all W atoms are dynamically disordered in the initial *Cmcm* phase and that there is a total ordering of the W atoms in the $P\bar{1}$ phase. The relatively large difference in the ΔS_1 values in $(NH_4)_2WO_2F_4$

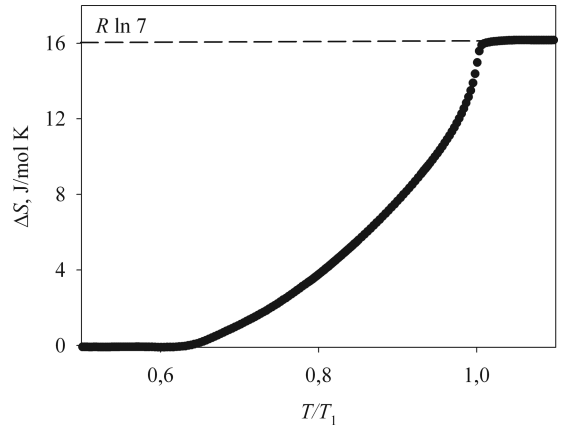

Figure 7. Temperature dependence of the excess entropy change on a scale of the reduced temperature T_1.

and $Rb_2MoO_2F_4$ indicates a significant role for the tetrahedral $[NH_4]$ groups in the mechanism of phase transitions in ammonium oxyfluorides $AA'MeO_2F_4$. In this case, it can be assumed that the decrease in the ΔS_1 value in $(ND_4)_2MoO_2F_4$ in comparison with $(NH_4)_2MoO_2F_4$ is associated with the change in the movement of the deuterated ammonium groups. In accordance with the single-crystal XRD data for $(NH_4)_2MoO_2F_4$,[6] only dynamically disordered MoO_2F_4 octahedra (56%) participate in the phase transition *Cmcm* ↔ *Pnma*. As for $[NH_4]$ groups, all of these were assumed to be disordered at two positions in the initial phase and totally ordered in the antiferroelectric phase. The entropy evaluated in the framework of this model agrees well with the value of ΔS_1 = 18.2 ± 1.3 J/mol·K ≈ R ln 8.9 determined experimentally.[7] Powder XRD data obtained on $(ND_4)_2MoO_2F_4$ showed disordering of the Mo atoms at four positions in the *Cmcm* phase and ordering in the *Pnma* phase.[9] Assuming that $[ND_4]$ groups are ordered in the initial phase and that only $[NH_4]$ groups (5%) contribute to the entropy of the phase transition, the value of ΔS_1 is equal to R ln 4 + R(2 × 0.05 ln 2) = 12.1 J/mol·K. The relatively small difference of this value compared to the experimental value of ΔS_1 = 15 ± 1 J/mol·K can be associated with the contribution from the displacements of the central atom as well as the partial ordering of some F/O atoms.[9]

According to the $T-p$ phase diagram for $(NH_4)_2MoO_2F_4$, an increase in the external hydrostatic pressure is accompanied by an increase in the T_1 temperature.[7] D → H substitution leads to a decrease in the unit cell volume of the G_0 phase and to an increase in T_1 [270 K (NH_4) → 272 K (ND_4)]. Thus, both of these peculiarities and the data in Table 1 show that the effects of the external and internal chemical pressures are similar. Using the dT_1/dp baric coefficient for $(NH_4)_2MoO_2F_4$, we estimated the change in the chemical pressure in $(ND_4)_2MoO_2F_4$ as $\Delta p \approx 0.02$ GPa.

Investigations of the $T-p$ phase diagram of $(ND_4)_2MoO_2F_4$ showed that the temperature range of the initial phase stability (space group *Cmcm*) was reduced under pressure. The baric coefficient dT_1/dp was increased by ∼25% compared to the protonated crystal (Table 1) and was found to be rather close to the value dT_1/dp = 110.5 K/GPa for the solid solution $(NH_4)_{1.8}Cs_{0.2}MoO_2F_4$.[13]

The phase transition at T_2 is of the displacement type (ΔS_2 ≈ 1.5 J/mol·K ≈ R ln 1.2), which is characteristic for all previously examined compounds $AA'MeO_2F_4$. This phase

DOI: 10.1021/acs.inorgchem.7b00811
Inorg. Chem. 2017, 56, 6706−6711

transition appears not to be directly related to the presence of the ammonium group in the structure. However, a study of the solid solutions $(NH_4)_{2-x}A_x'MoO_2F_4$ showed that the substitution of $NH_4 \rightarrow A'$ was accompanied by the appearance of hydrogen bonds, which led to a decrease in the T_2 temperature.[14]

Table 1 shows that deuteration leads to a slight increase in T_2 and a strong decrease in the baric coefficient dT_2/dp. As a result, the temperature range of the intermediate antiferroelectric phase (space group *Pnma*) in the $(ND_4)_2MoO_2F_4$ crystal expands with increasing pressure. The strong effect of D → H substitution on the susceptibility to external pressure was also observed in the related oxyfluoride $(NH_4)_2WO_2F_4$.[8] Because of the very large difference in the values of dT_1/dp and dT_2/dp, the triple point on the $T-p$ phase diagram of $(ND_4)_2WO_2F_4$ was observed at $p \approx 0.18$ GPa rather than ~0.7 GPa in the protonated crystal. In accordance with the baric coefficients (Table 1), the triple points on the $T-p$ phase diagram where the *Pnma* phase disappears can be realized in molybdenum compounds at a negative pressure of $p_{trp} \approx -1.2$ GPa in $(NH_4)_2MoO_2F_4$ and $p_{trp} = -0.8$ GPa in $(ND_4)_2MoO_2F_4$.

As for the origin of the phase transitions $A_2MoO_2F_4$ (A = NH_4, ND_4), it appears to be safe to say that this corresponds with the behavior of the dielectric properties. The common features in both crystals are a very broad temperature range of the change in ε below T_1, a relatively large difference between the ε values in the G_0 (space group *Cmcm*) and G_2 (space group *Pnma**) phases, and a lack of significant anomalies on the $\varepsilon(T)$ curve near T_2 except for a small inflection and a rather deep minimum in the tan $\delta(T)$ function at T_1. The almost nonanomalous behavior of ε in the vicinity of T_2 allows us to conclude that the G_2 phase is nonpolar in both $(ND_4)_2MoO_2F_4$ and $(NH_4)_2MoO_2F_4$. Moreover, second harmonic generation was not observed below T_2. In this case, the number of space groups suggested for the G_2 phase[9] can be reduced to two: *Pnma* and $P2_12_12_1$.

4. CONCLUSIONS

The heat capacity, thermal dilatation, susceptibility to hydrostatic pressure, and dielectric properties for the sequence of phase transitions G_0 (space group *Cmcm*) ↔ G_1 (space group *Pnma*) ↔ G_2 (space group *Pnma**) in the deuterated oxyfluoride compounds $(ND_4)_2MoO_2F_4$ (≈95% D) are carefully studied here and compared with those of a previously studied protonated crystal, $(NH_4)_2MoO_2F_4$.[9]

On the one hand, it was found that deuteration did not significantly change the temperatures of the structural transformations and qualitative behavior of the properties. On the other hand, D → H substitution led to rather marked differences in certain quantitative characteristics, as follows:

(1) The entropy change associated with the *Cmcm* ↔ *Pnma* phase transition remained typical for order−disorder processes but was somewhat decreased. This clearly indicates that ammonium groups play a significant role in the mechanism of structural distortions.

(2) The increase in the chemical pressure due to the decrease in the unit cell volume was accompanied by a decrease in the external hydrostatic pressure of the triple point and by the approach of the first-order *Cmcm* ↔ *Pnma* phase transition toward the tricritical point.

The virtually nonanomalous behavior of the dielectric properties in the vicinity of T_2, as well as an absence of second harmonic generation, allows us to assume that the G_2 phase is nonpolar; as a result, the number of space groups suggested for the G_2 phase[9] can be reduced to *Pnma* and $P2_12_12_1$.

AUTHOR INFORMATION

Corresponding Author

*E-mail:pepel@iph.krasn.ru.

ORCID

Evgeniy I. Pogoreltsev: 0000-0002-8583-0294

Notes

The authors declare no competing financial interest.

ACKNOWLEDGMENTS

We are grateful to A. G. Kocharova for preparation of the sample and Dr. A. M. Pugachev for examination of the second harmonic generation. This study was partially supported by the Russian Foundation for Basic Research (Project 16-32-00201 mol_a).

REFERENCES

(1) Gautier, R.; Gautier, R.; Chang, K. B.; Poeppelmeier, K. R. On the Origin of the Differences in Structure Directing Properties of Polar Metal Oxyfluoride $[MO_xF_{6-x}]^{2-}$ (x = 1, 2) Building Units. *Inorg. Chem.* **2015**, *54* (4), 1712−1719.

(2) Pogoreltsev, E. I.; Flerov, I. N.; Laptash, N. M. Dielectric Properties and Phase Transitions in Some Oxyfluorides with the MeO_xF_{6-x} (x = 1, 2, 3) Anion in Structure. *Ferroelectrics* **2010**, *401*, 207−210.

(3) Welk, M. E.; Norquist, A. J.; Stern, C. L.; Poeppelmeier, K. R. The ordered $[WO_2F_4]^{2-}$ anion. *Inorg. Chem.* **2001**, *40*, 5479−5480.

(4) Flerov, I. N.; Fokina, V. D.; Gorev, M. V.; Vasiliev, A. D.; Bovina, A. F.; Molokeev, M. S.; Kocharova, A. G.; Laptash, N. M. Mechanism of phase transitions in the $(NH_4)_2WO_2F_4$ ferroelastic. *Phys. Solid State* **2006**, *48* (4), 759−764.

(5) Udovenko, A. A.; Laptash, N. M. Disorder in crystals of dioxofluorotungstates, $(NH_4)_2WO_2F_4$ and $Rb_2WO_2F_4$. *Acta Crystallogr., Sect. B: Struct. Sci.* **2008**, *64*, 645−651.

(6) Udovenko, A. A.; Vasiliev, A. D.; Laptash, N. M. Orientational disorder and phase transitions in crystals of dioxofluoromolybdate, $(NH_4)_2MoO_2F_4$. *Acta Crystallogr., Sect. B: Struct. Sci.* **2010**, *66*, 34−39.

(7) Fokina, V. D.; Bogdanov, E. V.; Pogorel'tsev, E. I.; Bondarev, V. S.; Flerov, I. N.; Laptash, N. M. Calorimetric and dielectric studies of the $(NH_4)_2MoO_2F_4$ oxyfluoride. *Phys. Solid State* **2010**, *52* (1), 158−166.

(8) Flerov, I. N.; Fokina, V. D.; Gorev, M. V.; Bogdanov, E. V.; Molokeev, M. S.; Bovina, A. F.; Kocharova, A. G. Effect of deuteration on the thermal properties and structural parameters of the $(NH_4)_2WO_2F_4$ oxyfluoride. *Phys. Solid State* **2007**, *49* (6), 1149−1156.

(9) Bogdanov, E. V.; Mel'nikova, S. V.; Pogoreltsev, E. I.; Molokeev, M. S.; Flerov, I. N. The structure and phase transitions in oxyfluoride $(ND_4)_2MoO_2F_4$. *Solid State Sci.* **2016**, *61*, 155−160.

(10) Bogdanov, E. V.; Pogoreltsev, E. I.; Mel'nikova, S. V.; Gorev, M. V.; Flerov, I. N.; Molokeev, M. S.; Kartashev, A. V.; Kocharova, A. G.; Laptash, N. M. Investigation into phase diagrams of the fluorine-oxygen system: Ferroelastic-antiferroelectric $(NH_4)_2WO_2F_4$-$(NH_4)_2MoO_2F_4$. *Phys. Solid State* **2013**, *55* (2), 409−418.

(11) Flerov, I. N.; Gorev, M. V.; Aleksandrov, K. S.; Tressaud, A.; Grannec, J.; Couzi, M. Phase Transitions in Elpasolites. *Mater. Sci. Eng., R* **1998**, *24*, 81−151.

(12) Aleksandrov, K. S.; Flerov, I. N. The applications of the thermodynamic theory to structural phase transitions close to the tricritical point. *Fiz. Tverd. Tela.* **1979**, *21*, 327−336.

(13) Bogdanov, E. V.; Vasil'ev, A. D.; Flerov, I. N.; Laptash, N. M. Effect of cation substitution in fluorine-oxygen molybdates $(NH_4)_{2-x}A_xMoO_2F_4$. *Phys. Solid State* **2011**, *53* (2), 303−308.

DOI: 10.1021/acs.inorgchem.7b00811
Inorg. Chem. 2017, 56, 6706−6711

(14) Mel'nikova, S. V.; Laptash, N. M. Optical studies of the (T-x) phase diagram of oxyfluoride $(NH_4)_2MoO_2F_4$-$Rb_2MoO_2F_4$ solid solutions. *Phys. Solid State* **2015**, *57* (6), 1201−1205.

DOI: 10.1021/acs.inorgchem.7b00811
Inorg. Chem. 2017, 56, 6706−6711